



Open photoacoustic cell for concentration measurements in rapidly flowing gas

János Fekete^a, Péter Torma^{b,c}, Anna Szabó^{a,b}, Miklós Balogh^d, Csaba Horváth^d,
Tamás Weidinger^e, Gábor Szabó^a, Zoltán Bozóki^{a,b,*}

^a Department of Optics and Quantum Electronics, University of Szeged, H-6720 Szeged, Hungary

^b ELKH-SZTE Research Group for Photoacoustic Monitoring of Environmental Processes, H-6720 Szeged, Hungary

^c National Laboratory for Water Science and Water Security, Budapest University of Technology and Economics, Faculty of Civil Engineering, Department of Hydraulic and Water Resources Engineering, H-1111 Budapest, Hungary

^d Department of Fluid Mechanics, Faculty of Mechanical Engineering, Budapest University of Technology and Economics, H-1111 Budapest, Hungary

^e Department of Meteorology, Eötvös Loránd University, H-1117 Budapest, Hungary

A B S T R A C T

High temporal resolution concentration measurements in rapid gas flows pose a serious challenge for most analytical instruments. The interaction of such flows with solid surfaces can generate excessive aero-acoustic noise making the application of the photoacoustic detection method seemingly impossible. Yet, the fully open photoacoustic cell (OC) has proven to be operable even when the measured gas flows through it at a velocity of several m/s. The OC is a slightly modified version of a previously introduced OC based on the excitation of a combined acoustic mode of a cylindrical resonator. The noise characteristics and analytical performance of the OC are tested in an anechoic room and under field conditions. Here we present the first successful application of a sampling-free OC for water vapor flux measurements.

1. Introduction

Extractive sampling-based measurements are notoriously vulnerable to gas sampling errors. This is especially true for aerosol analysis, where reliable measurements require the strict maintenance of isokinetic sampling conditions, i.e. the velocity of the gas entering a sample gas transmission system must be equal to that of the undisturbed gas stream. Isokinetic sampling is not critical for gaseous analytes, yet temporal or even permanent differences might appear between the measured and actual analyte concentrations due to the occurrence of adsorption/desorption processes (ADP) in the sampling system and the detection unit. These errors can be decreased by using properly selected materials and coatings for these units. Alternatively, the effects of ADP can also be measured and incorporated into a model that describes the response of the sampling unit. Additionally, the temporal variation of the input concentration can be determined by a system theory approach, i.e., by deconvolving the measured signal with the transfer function of the sampling unit. Another drawback of extractive sampling is that it inevitably increases the response time of the measurement. Transfer through the sampling and the detection units can be quantified by a residence time distribution function [1]. The first moment of residence

time distribution is the response time, which can be approximated with the purging time calculated as the combined volume of the sampling and the detection units divided by the volumetric flow rate of the sampled gas. To allow a detection unit to follow sudden concentration variations with short delays and minimal signal distortion, the volumes of the sampling and detection units need to be minimized and the volumetric flow rate of the sampled gas must be maximized. However, various secondary effects, including “dead volumes” and ADP, prolong the response of the system to sudden concentration variations.

Flux measurements for studying surface-atmosphere exchange processes is a research field in which the use of extractive sampling-based analytical instruments is especially problematic. Among different analytes targeted in flux measurements, water vapor is key as evapotranspiration plays a central role in the hydrological cycle by transferring water vapor into the atmosphere and regulating the energy balance of the surface. Eddy covariance (EC) is a widely used micrometeorological technique to monitor the water vapor exchange between the atmosphere and various surfaces. It is a direct measurement method routinely used to record surface layer fluxes [2]. An EC instrument typically consists of a three-dimensional sonic anemometer and a gas analyzer that measure and analyze the horizontal and vertical wind components, as well as

* Correspondence to: Department of Optics and Quantum Electronics, University of Szeged, Dom ter 9., H-6720 Szeged, Hungary.

E-mail address: zbozoki@physx.u-szeged.hu (Z. Bozóki).

<https://doi.org/10.1016/j.pacs.2023.100469>

Received 14 December 2022; Received in revised form 24 February 2023; Accepted 24 February 2023

Available online 26 February 2023

2213-5979/© 2023 The Authors. Published by Elsevier GmbH. This is an open access article under the CC BY-NC-ND license (<http://creativecommons.org/licenses/by-nc-nd/4.0/>).

fluctuations in gas concentrations (e.g., water vapor) [3]. These variables must be sampled at a high frequency (typically at 10 Hz), and the obtained profile can be used to derive the surface fluxes [4]. Accordingly, the water vapor flux can be calculated as follows:

$$F_{\rho_v} = \overline{w' \rho_v'} \quad (1)$$

where w' and ρ_v' are the fluctuations of vertical wind speed and water vapor density around their respective means during a chosen averaging period (typically ranging from 5 min to a few hours). The overbar denotes the covariance of these two quantities.

Depending on the gas of interest, EC measurements can be conducted with a wide variety of fast-response sensors having either an open- or a closed-path (i.e., extractive sampling based) configuration. In the latter case, the air is delivered to the gas analyzer through a tube, which leads to the attenuation of concentration fluctuations due to the flow within the tube [5]. In contrast, open-path sensors provide a sampling-free approach with minimal disturbance and direct gas concentration measurement [6]. In the case of water vapor, infrared (IR) sensors are dominantly used in both open- and closed-path systems, although other measurement principles can also be applied. Water vapor concentration has also been successfully measured by proton-transfer-reaction mass spectrometry; however, this technique requires a closed-path system.

Sampling-free methods are based either on miniaturized sensors which can be immersed directly into the flowing gas or on open-path systems through which the measured gas can flow. Quite uniquely, photoacoustic (PA) cells can be optimized for either approach [7–10] because the PA signal generated by the absorption of periodically modulated light beam can be maximized in two ways:

- A non-resonant PA cell can have an inner volume of a few cm^3 or less. As the PA signal is inversely proportional both to the volume of the cell and to the modulation frequency, strong PA signals can be generated in such a cell whenever its light source is modulated at a low frequency (typically at a few Hz). Due to its small size, this type of cell can be immersed directly into the measured gas stream [11].
- A resonant PA cell has a high volume (several tens or hundreds of cm^3) and its light source is typically modulated in the kHz range. In this case, the strength of the PA signal is ensured by the quality factor of the resonance (Q), which can be as high as 200 [12]. These cells can be constructed in a way that the measured gas flows through it freely, while the its Q factor suffers a tolerable decrease only.

While most of the analytical parameters of the two types of PA cells can be rather similar, resonant PA cells clearly outperform their non-resonant counterparts as far as response time is concerned, primarily because the gas enters these cells by direct flow or via the much slower process of diffusion. Nevertheless, even for a resonant PA cell the envisioned sub-second response time can only be achieved in an open-path construction, i.e. the use of extractive sampling must be completely avoided (see below). The consequences of having an open resonator are the reduction of the Q factor and that the resonator is directly exposed to external acoustic noise. Therefore, great emphasis should be put on the optimization of the resonator design and of the excited acoustic mode [13–15].

In this paper, we present the first field application of our initial open PA cell (OC) concept, which we developed about a decade ago [16]. Regarding the maximization of the PA signal, the applied concept is the same for both the original and the upgraded version of the OC. The PA signal is generated by exciting the combined mode of the second azimuthal and the first longitudinal modes (0,2,1). Furthermore, the external noise is suppressed with the same method i.e. by placing two microphones into the resonator in a way that they sense the same acoustic resonance, but in opposite phases. The output signals of these two microphones are fed into a differential amplifier, which efficiently subtracts the noise that impinges on the microphones in the same phase,

while the subtraction doubles the useful PA signal, due to the opposite phase of the excited resonance recorded at the positions of the two microphones.

The aim of the present paper was to study, for the first time, the disturbance of the gas flow and response time of the OC. This article presents the first successful application of a sampling-free OC for water vapor flux measurement. Section 2 contains the description of the OC-based water vapor measuring PA system and its tests conducted both in an anechoic room and under field conditions. Section 3 presents and discusses the measurement results in combination with some theoretical considerations, while Section 4 provides conclusions of our work.

2. Experimental

The OC presented here is a slightly modified version of our previous OC, which had an eigenfrequency of approximately 10.5 kHz for (0,2,1) eigenmode (length 32 mm, radius 17 mm) [16]. The novel cylindrical acoustic resonator has a length and radius of 50 mm and 14 mm, respectively, resulting in an approximate eigenfrequency of 12.5 kHz. The increase of the eigenfrequency is advantageous as environmental acoustic noises typically have $1/f$ frequency dependence. An additional upgrade in the current OC is the replacement of the formerly used electret microphones with MEMS microphones (Sisonic™ SPU0410HR5H-PB). For the excitation of the PA signal with an amplitude proportional to the water vapor concentration, a near-infrared pigtailed butterfly diode laser (NLK1E5GAAA, NTT Electronics, with an output power of about 20 mW) is used. It is tuned to 1371 nm, where water vapor has a strong absorption line. Laser control and modulation, microphone signal collection, amplification, and PA signal calculation are performed with special electronics (courtesy of Videoton Holding Plc.) as described previously in numerous publications [17].

The acoustic characteristics of the OC were measured in the anechoic room of the Békésy György Acoustic Research Laboratory (Budapest). Gas flows through the OC at different velocities were generated with a special flow system which, due to the incorporated silencers, generates negligible flow noise. Noise spectra generated aero-acoustically within the OC were recorded by the OC's microphones operated in differential mode and were analyzed by the data acquisition unit of the Videoton electronics. As a noise level calibration reference, we used a Brüel & Kjaer microphone (type 4165) and its electronics (type 2639 preamplifier, type 2636 amplifier) in these noise measurements. Our goal with these measurements was to find the highest flow velocity with which the OC is still operable and to verify the applicability of the numerical model developed for the simulation of the aero-acoustical noise generated by the interaction of the flow and the OC. In these numerical experiments, a block structured, high resolution mesh was produced in a way to satisfy the requirements of low-Reynolds wall treatment ($y^+ < 1$). Only a quarter of the original geometry was modeled, supposing tangential periodicity. Assuming a low Mach number ($Ma < 0.05$), we applied an incompressible approach using aero-acoustic analogies. The numerical investigations were conducted in three steps using the OpenFOAM toolbox [18]. First, we performed a steady state precursor simulation with an axially periodic domain modeling an infinitely long upwind pipe section, using the Launder-Sharma $k-\epsilon$ Low-Reynolds turbulence model. The flow was driven by a pressure gradient, which was iteratively tuned to reach the desired volume flow rate. In the next step, we generated the initial conditions by running a steady state simulation on OC geometry, taking the results of the precursor simulation as inlet boundary conditions, applying the same turbulence model. In the last step, we ran a time resolved simulation using the initial and boundary conditions generated by the previous simulations. At this stage, we used a hybrid turbulence modeling approach, the Spalart-Allmaras Detached Eddy Simulation (DES) model, which combines the advantages of Large Eddy Simulation and Reynolds averaged models. Furthermore, we determined the time resolved boundary conditions at the inlet with the Divergence-Free Synthetic Eddy Method [19]. Finally, and we tested the OC for water

vapor flux measurements over a plain grassland in a short, few-hour-long measurement campaign. A commercial EC instrument – consisting of a CSAT3 sonic anemometer (Campbell Sci. Ltd.) and an EC150 IR gas analyzer (Campbell Sci. Ltd.) which measured the vertical wind speed and water vapor density fluctuations, respectively – was supplemented with the OC installed as close as possible to the EC instruments. A CR3000 Datalogger (Campbell Sci. Ltd.) collected the data of the anemometer and the IR analyzer in a synchronized manner. The signal of the OC was recorded separately. Fluctuation components were determined by decomposing the velocity and scalar time series of concentrations into means and deviations around the means. Turbulent water vapor fluxes were calculated by Eq. 1, in which water vapor density fluctuations were obtained either from the IR gas analyzer or the OC. The flux data calculated from the readings of the IR sensor were considered as reference. The averaging periods for both flux measurements were 15 min. Relative to the data of the IR sensor, temporal lags may occur between the w' and the ρ_v' time series from the OC, as it was positioned further away from the anemometer and its recordings were not synchronized with the wind speed measurements. To obtain correct fluxes from the OC measurements, the time delay between the w' and ρ_v' time series must be corrected. An accepted method for time delay adjustment is covariance maximization [20,21]. Using this method, we shifted one of the time series relative to the other one in both directions, scan by scan, until we found the maximum covariance ($w'\rho_v'$). Then we compared the fluxes obtained from the two gas sensors based on their co-spectra. The co-spectrum represents the contribution of different eddies to the total flux along their frequencies and is defined as the product of the Fourier transform of w' and the complex conjugate of the Fourier transform of ρ_v' . The total flux can also be calculated by integrating the one-sided co-spectrum over frequency. In this first analysis, we compared raw fluxes and did not perform any further corrections which may be required in standard EC measurements [22].

3. Results and discussions

Under the same measurement conditions, i.e., by using the same laser and measuring the same concentration of water vapor, the current OC was found to generate a PA signal approximately 5 times higher than the old OC. This unexpected sensitivity increase corresponds to an increase in the Q factor of the excited resonance ($Q \approx 50$ and $Q \approx 10$ for the current and the old OC, respectively). This development can be attributed to the changes of the geometrical parameters and the type of the attached microphones.

The level of the generated noise detected during the anechoic room measurements was found to be proportional to the flow velocity raised to the power of 6.27, which shows the presence of predominantly dipole sound sources [23]. This steep increase means that there is a rather sharp threshold in flow velocity; below this threshold the flow-generated noise is buried by the self-noise of the microphones, while above it the aero-acoustic noise hinders the PA measurements. We found this threshold flow velocity to be at about 4 m/s, above which we observed a supposedly mechanical overload in the microphone signals. Fig. 1 shows the result of noise measurement in the anechoic room at a flow velocity of 4 m/s together with the result of the numerical aero-acoustic noise simulation. The yielded Sound Pressure Level (SPL) is shown in Fig. 1, together with the measured reference. The fact that the measured and simulated data show good agreement verifies the simulation, and furthermore opens the possibility of using the numerical model for further optimization of the aero-acoustic properties of the OC in the future.

Although the field test of the OC for water vapor detection could not cover a wide range of meteorological conditions from low to high wind speeds with different atmospheric stability states, these first results have satisfactorily demonstrated the applicability of the OC for water vapor flux measurements. With the covariance maximization procedure, we

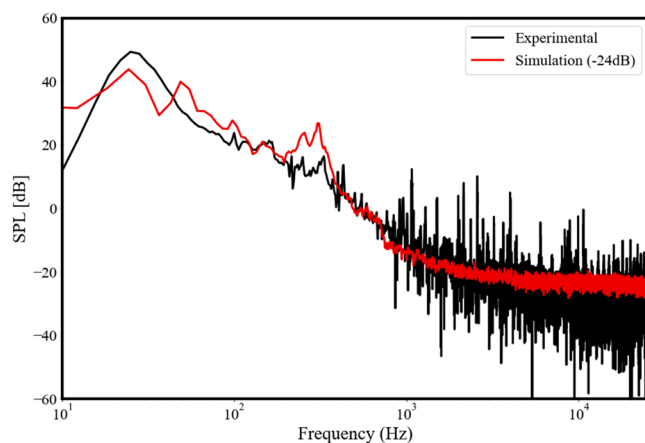


Fig. 1. Sound Pressure Level (SPL) of aero-acoustic noise as a function of frequency obtained from experiments (black line) and numerical simulations (red line). Experiments were carried out in the anechoic room of the Békésy György Acoustic Research Laboratory using the microphones of the OC.

could identify a clear maximum in the calculated raw fluxes for the OC. Similarly to the covariance maximization procedure in the case of the OC, covariances were also calculated as a function of time shift (Δt) using the IR sensor data. As Fig. 2 shows, the covariance functions of the OC and the IR sensors properly overlap. This indicates that the OC can capture the ρ_v' variations with an accuracy comparable to that of the IR sensor.

In Fig. 3, the co-spectra (from which total fluxes can be calculated by integration) are compared when the time series were transformed from time domain into frequency domain, showing how much flux is transported at each frequency. We observed that at low frequencies, the OC data based co-spectrum was in good agreement with the one obtained from the IR sensor, and it also followed the theoretical spectrum in the upper part of the inertial sub-range. The inertial sub-range is at intermediate frequencies where turbulence is isotropic. In this range, turbulent eddies are transformed into smaller ones following an energy cascade. According to Kolmogorov's law, the energy decrease occurs with increasing frequency (f) proportional to $f^{-5/3}$ [4]. However, the PA system somewhat underestimated the flux portion at higher frequencies. This deviation may be attributed to several reasons, e.g. the shape and orientation of the OC were not optimal; the distance from the anemometer was larger than in the case of the IR sensor. This latter problem is often referred to as sensor separation. Furthermore, it is also common in EC measurements that even fast-response IR scalar sensors provide attenuations at frequencies above 1 Hz as they cannot perfectly

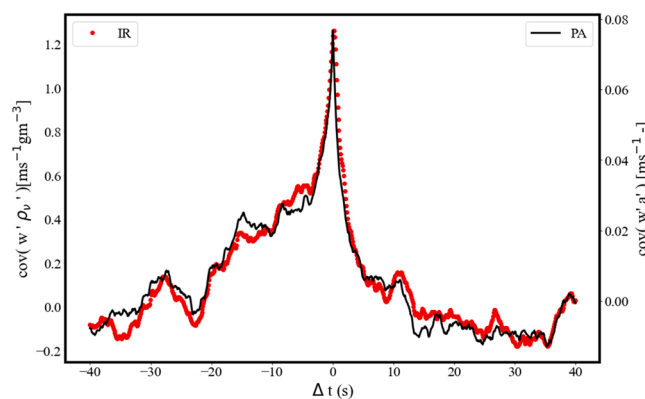


Fig. 2. Covariance values obtained by shifting water vapor fluctuation (ρ_v') time series from the IR sensor (red dots) and PA signal fluctuation (α') from the PA sensor (solid black line) relative to the vertical wind velocity fluctuation (w') as a function of time shift (Δt).

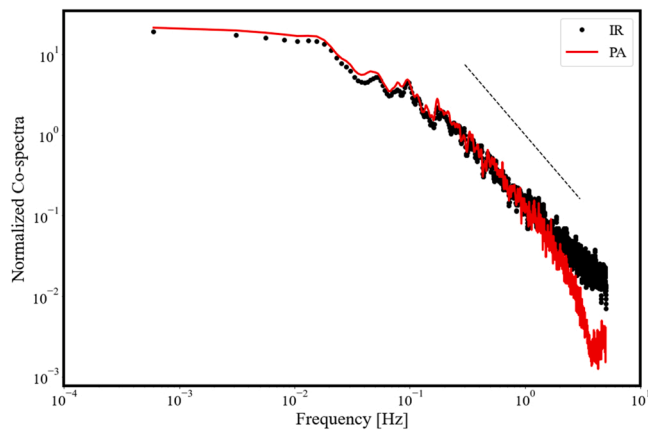


Fig. 3. Logarithmic co-spectra normalized by the flux by the IR (dots) and PA (solid red line) sensors. The dashed line shows the theoretical slope ($f^{-5/3}$) in the inertial subrange.

detect small-scale variations related to eddies with smaller wavelengths [24].

As co-spectrum calculation is a fundamental step in standardized EC postprocessing procedures, various analytical (theoretical) and empirical corrections exist to compensate for losses in different frequency ranges depending on the scalar variable [22,25]. In the case of water vapor flux, an accepted method for the correction of high-frequency attenuation is the application of empirical spectral transfer functions [6,24,26]. These functions can be derived by employing theoretical or empirical loss-free spectra (i.e., sensible heat flux). Following the literature, for this short test period, we could establish an empirical transfer function based on the obtained IR and EC co-spectrum pairs to compensate for the spectral loss and resulted in good agreement with the IR-based water vapor fluxes. Furthermore, with longer field tests under more diverse meteorological conditions and possibly also with various OC orientations and/or aerodynamic properties, more optimal measurement configurations are expected to be found.

The reported field measurements open the possibility to estimate the response time of the OC, which obviously depends on gas flow speed. As the roughest estimation, one can divide the length of the OC by the gas flow velocity to give the first estimate of the response time. In case of a wind speed of 1 m/s, this estimated response time is 50 ms. As a more systematic approach one can define an empirical transfer function, which is the ratio of the dampened (PA) and the undampened (IR) co-spectra [24,27]. This can also be described by the transfer function of a first-order sensor, as follows [28]:

$$H_{wa}(f) \equiv \frac{Co_{PA}(f)}{Co_{IR}(f)} = \frac{1}{1 + (2\pi\tau_c f)^2} \quad (2)$$

where $Co_{PA}(f)$ and $Co_{IR}(f)$ are the co-spectra from the IR gas analyzer and the OC, respectively, and f is the frequency. The right-hand side term of Eq. 2 is the transfer function of a first-order instrument, where τ_c is the characteristic time constant of the sensor response [24]. As shown in Fig. 4, the obtained empirical transfer function followed reasonably well the theoretical first-order transfer function, representing a sensor response of 10 Hz or $\tau_c = 0.1$ s. This estimated time constant of the OC is an order of magnitude better than that of the proton-transfer-reaction mass spectrometry, which could be characterized by $\tau_c = 1.2$ s [26]. Obviously, to improve our understanding of the time constant and the temporal response of the OC, we must conduct tests under diverse meteorological conditions, e.g., at higher wind speeds. Indeed, the characteristic time constant of sensor response is known to be affected by atmospheric stability and wind speed [26,28].

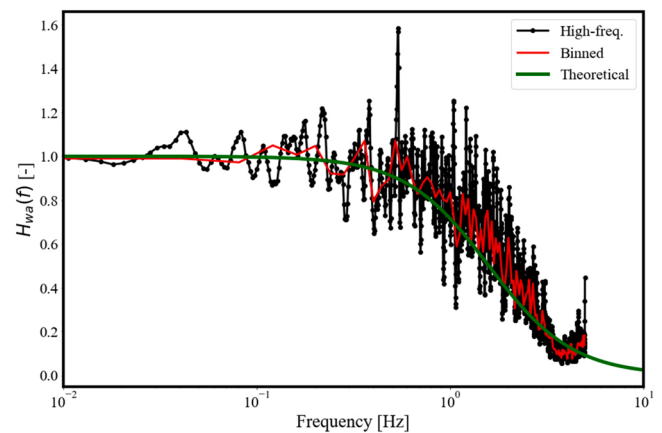


Fig. 4. Comparison of the theoretical (solid green line) and the empirical (circles – high-frequency data, solid red line – binned medians) transfer functions for the high-frequency damping correction for a sample, 15 min period.

4. Conclusions

An OC-based on the excitation of a combined acoustic mode of a cylindrical resonator was upgraded and tested in an anechoic room and under field conditions. During anechoic room measurements, the threshold flow velocity was found to be approximately 4 m/s. This relatively high flow velocity value indicated the suitability of our OC for field measurements. In terms of the flux measurements, the OC provided not just promising but reliable estimates. In combination with a sonic anemometer, it constitutes an open-path EC arrangement having unambiguous benefits compared to an extractive sampling-based closed-path system and is expected to result in a flux sensor with low disturbance against turbulent airflow. Based on the first results, the application of an empirical spectral correction function may be necessary, but this is a standard procedure in EC measurements. Overall, we firmly believe that the combination of the presented OC with a small sonic anemometer (e.g., TriSonica Sphere Wind Flux sensor) will lead to an EC setup suitable for installation on unmanned aerial vehicles like drones.

Declaration of Competing Interest

The authors declare that they have no known competing financial interests or personal relationships that could have appeared to influence the work reported in this paper.

Data availability

Data will be made available on request.

Acknowledgments

The work was supported by the National Research, Development and Innovation Office (NKFIH): project number OTKA-K-138176 and the Széchenyi Plan Plus program with the support of the RRF 2.3.1 21 2022 00008 project.

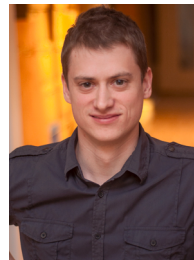
References

- [1] Z. Bozóki, T. Guba, T. Ajtai, A. Szabó, G. Szabó, Photoacoustic detection based permeation measurements: case study for separation of the instrument response from the measured physical process, *Photoacoustics* 12 (2018) 1–5, <https://doi.org/10.1016/j.pacs.2018.08.001>.
- [2] D. Baldocchi, E. Falge, L. Gu, R. Olson, D. Hollinger, S. Running, P. Anthoni, C. Bernhofer, K. Davis, R. Evans, J. Fuentes, A. Goldstein, G. Katul, B. Law, X. Lee, Y. Malhi, T. Meyers, W. Munger, W. Oechel, U.K.T. Paw, K. Pilegaard, H.P. Schmid, R. Valentini, S. Verma, T. Vesala, K. Wilson, S. Wofsy, FLUXNET: a new tool to study the temporal and spatial variability of ecosystem-scale carbon dioxide, water

- vapor, and energy flux densities, *Bull. Am. Meteorol. Soc.* 82 (2001) 2415–2434, [https://doi.org/10.1175/1520-0477\(2001\)082<2415:FANITTS>2.3.CO;2](https://doi.org/10.1175/1520-0477(2001)082<2415:FANITTS>2.3.CO;2).
- [3] G. Lükő, P. Torma, T. Weidinger, T. Krämer, Air-lake momentum and heat exchange in very young waves using energy and water budget closure, *J. Geophys. Res. Atmos.* 127 (2022), <https://doi.org/10.1029/2021JD036099>.
- [4] T. Foken, *Micrometeorology*, Springer-Verlag, Berlin, 2008.
- [5] W.J. Massman, The attenuation of concentration fluctuations in turbulent flow through a tube, *J. Geophys. Res.* 96 (1991) 15269, <https://doi.org/10.1029/91JD01514>.
- [6] P. Polonik, W.S. Chan, D.P. Billesbach, G. Burba, J. Li, A. Nottrott, I. Bogoev, B. Conrad, S.C. Biraud, Comparison of gas analyzers for eddy covariance: effects of analyzer type and spectral corrections on fluxes, *Agric. For. Meteorol.* 272–273 (2019) 128–142, <https://doi.org/10.1016/j.agrformet.2019.02.010>.
- [7] T. Strahl, J. Steinebrunner, C. Weber, J. Wöllenstein, K. Schmitt, Photoacoustic methane detection inside a MEMS microphone, *Photoacoustics* (2022), 100428, <https://doi.org/10.1016/j.pacs.2022.100428>.
- [8] T. Wei, H. Wu, L. Dong, F. Tittel, Acoustic detection module design of a quartz-enhanced photoacoustic sensor, *Sensors* 19 (2019) 1093, <https://doi.org/10.3390/s19051093>.
- [9] A. Sampaolo, P. Patimisco, M. Giglio, A. Zifarelli, H. Wu, L. Dong, V. Spagnolo, Quartz-enhanced photoacoustic spectroscopy for multi-gas detection: a review, *Anal. Chim. Acta* 1202 (2022), 338894, <https://doi.org/10.1016/j.aca.2021.338894>.
- [10] P. Patimisco, A. Sampaolo, L. Dong, F.K. Tittel, V. Spagnolo, Recent advances in quartz enhanced photoacoustic sensing, *Appl. Phys. Rev.* 5 (2018), 011106, <https://doi.org/10.1063/1.5013612>.
- [11] J. Huber, C. Weber, A. Eberhardt, J. Wöllenstein, Photoacoustic CO₂-sensor for automotive applications, *Procedia Eng.* 168 (2016) 3–6, <https://doi.org/10.1016/j.proeng.2016.11.111>.
- [12] A. Miklós, P. Hess, Z. Bozóki, Application of acoustic resonators in photoacoustic trace gas analysis and metrology, *Rev. Sci. Instrum.* 72 (2001) 1937–1955, <https://doi.org/10.1063/1.1353198>.
- [13] B. Lang, A. Bergmann, Design framework for a gas sensor based on an open photoacoustic resonator, in: 2016 IEEE Sens., IEEE, Orlando, FL, USA, 2016: pp. 1–3. <https://doi.org/10.1109/ICSENS.2016.7808433>.
- [14] S. El-Busaidy, B. Baumann, M. Wolff, L. Duggen, Shape optimization of an open photoacoustic resonator, *Appl. Sci.* 11 (2021) 2571, <https://doi.org/10.3390/app11062571>.
- [15] S.A.S. El-Busaidy, B. Baumann, M. Wolff, L. Duggen, Modelling of open photoacoustic resonators, *Photoacoustics* 18 (2020), 100161, <https://doi.org/10.1016/j.pacs.2020.100161>.
- [16] Z. Bozóki, A. Szabó, A. Mohácsi, G. Szabó, A fully opened photoacoustic resonator based system for fast response gas concentration measurements, *Sens. Actuators B Chem.* 147 (2010) 206–212, <https://doi.org/10.1016/j.snb.2010.02.060>.
- [17] Z. Bozóki, A. Pogány, G. Szabó, Photoacoustic instruments for practical applications: present, potentials, and future challenges, *Appl. Spectrosc. Rev.* 46 (2011) 1–37, <https://doi.org/10.1080/05704928.2010.520178>.
- [18] H.G. Weller, G. Tabor, H. Jasak, C. Fureby, A tensorial approach to computational continuum mechanics using object-oriented techniques, *Comput. Phys.* 12 (1998) 620, <https://doi.org/10.1063/1.168744>.
- [19] R. Poletto, T. Craft, A. Revell, A new divergence free synthetic eddy method for the reproduction of inlet flow conditions for LES, *Flow. Turbul. Combust.* 91 (2013) 519–539, <https://doi.org/10.1007/s10494-013-9488-2>.
- [20] George Burba Eddy Covariance Method for Scientific, Regulatory, and Commercial Applications, LI-COR Biosciences, Lincoln, Nebraska, 2022.
- [21] K.-M. Kohonen, P. Kolari, L.M.J. Kooijmans, H. Chen, U. Seibt, W. Sun, I. Mammarella, Towards standardized processing of eddy covariance flux measurements of carbonyl sulfide, *Atmos. Meas. Tech.* 13 (2020) 3957–3975, <https://doi.org/10.5194/amt-13-3957-2020>.
- [22] S. Sabbatini, I. Mammarella, N. Arriga, G. Fratini, A. Graf, L. Hörtnagl, A. Ibrom, B. Longdoz, M. Mauder, L. Merbold, S. Metzger, L. Montagnani, A. Pitacco, C. Rebmann, P. Sedláč, L. Šigut, D. Vitale, D. Papale, Eddy covariance raw data processing for CO₂ and energy fluxes calculation at ICOS ecosystem stations, *Int. Agrophys.* 32 (2018) 495–515, <https://doi.org/10.1515/intag-2017-0043>.
- [23] S. Glegg, W. Devenport, Chapter 4 - Lighthill's acoustic analogy, in: S. Glegg, W. Devenport (Eds.), *Aeroacoustics Low Mach Number Flows*, Academic Press, 2017, pp. 73–93, <https://doi.org/10.1016/B978-0-12-809651-2.00004-7>.
- [24] T.W. Horst, A simple formula for attenuation of eddy fluxes measured with first-order-response scalar sensors, *Bound. -Layer. Meteorol.* 82 (1997) 219–233, <https://doi.org/10.1023/A:1000229130034>.
- [25] W.J. Massman, R. Clement, Uncertainty in Eddy covariance flux estimates resulting from spectral attenuation, in: *Handb. Micrometeorology*, Kluwer Academic Publishers, Dordrecht, 2004, pp. 67–99, https://doi.org/10.1007/1-4020-2265-4_4.
- [26] C. Ammann, A. Brunner, C. Spirig, A. Neffel, Technical note: Water vapour concentration and flux measurements with PTR-MS, *Atmos. Chem. Phys.* 6 (2006) 4643–4651, <https://doi.org/10.5194/acp-6-4643-2006>.
- [27] W.J. Massman, A simple method for estimating frequency response corrections for eddy covariance systems, *Agric. For. Meteorol.* 104 (2000) 185–198, [https://doi.org/10.1016/S0168-1923\(00\)00164-7](https://doi.org/10.1016/S0168-1923(00)00164-7).
- [28] H. Su, H.P. Schmid, C.S.B. Grimmond, C.S. Vogel, A.J. Oliphant, Spectral characteristics and correction of long-term Eddy-covariance measurements over two mixed hardwood forests in non-flat terrain, *Bound. -Layer. Meteorol.* 110 (2004) 213–253, <https://doi.org/10.1023/A:1026099523505>.



János Fekete received his MSc degree in physics at University of Szeged in 2020. He has been working at the University of Szeged from 2018 to present. He is a Ph.D. student since 2020 at University of Szeged. He is working on development of photoacoustic instruments and measurement technics applied in gas phase.



Péter Torma received his MSc and Ph.D. degrees in civil engineering in 2011 and 2016. He has been working at the Dept. of Hydraulic and Water Resources Engineering at Budapest University of Technology and Economics from 2011 to the present, since 2019, as an associate professor. He was a visiting researcher at UW-Madison (USA) for ten months as a Fulbright Scholar in the academic year of 2017/2018. His research fields and interests include physical limnology, hydrometeorology, turbulent exchange processes at the air-water interface, eddy-covariance measurements, and numerical hydrodynamic modeling.



Anna Szabó received her M.Sc. and Ph.D. degrees in physics in 2010 and 2016, respectively. She has been working at University of Szeged from 2013 to present. Since 2022 she is a research fellow of the ELKH-SZTE Research Group for Photoacoustic Monitoring of Environmental Processes. Her research interest includes photoacoustic spectroscopy based gas analysis for medical research and environmental monitoring.



Miklós Balogh received his M.Sc. degree in meteorology at ELTE, Faculty of Science in 2006, his Research Master degree in Fluid Dynamics at the Von Kármán Institute (VKI) in 2010, and his Ph.D. degree in Mechanical Engineering at the Budapest University of Technology and Economics (BME) in 2015. He has been working in the Department of Fluid Mechanics at the BME from 2011 to present, since 2015 as an assistant professor. His research fields and interests include turbulence modeling, model development and CFD solver development for the simulation of atmospheric flows, pore-scale flows, furthermore for problems in aerodynamics and aeroacoustics.



Csaba Horváth received a Ph.D. in mechanical engineering in 2015 from the Budapest University of Technology and Economics. He is currently an associate professor and deputy head of department at the Department of Fluid Mechanics of the Faculty of Mechanical Engineering at the Budapest University of Technology and Economics. He is also deputy principal of the BME-AUDI Hungaria Cooperative Research Center (BME-AUDI K3) at the university. His main field of interest within fluid mechanics is turbomachinery aerodynamics and aeroacoustics. Together with his team he works on many R+D projects which are supported by government grants as well as industrial partners.



Tamás Weidinger received his M.Sc. and Ph.D. degrees in Meteorology in 1983 and 1992, respectively. He has been working at the Eötvös Loránd University, Department of Meteorology from 1983 up to date, and from 2013 as a habilitate associate professor. His main areas of education are general meteorology, micrometeorology, and dynamic meteorology. His main fields of research are boundary-layer meteorology, measurement and modeling of surface energy budget components and trace gas fluxes (especially ozone and ammonia). He is an editor of the Theoretical and Applied Climatology Journal, and Editorial Board member of *Időjárás*, Quarterly Journal of the Hungarian Meteorological Service.



Zoltán Bozóki received his M.Sc., Ph.D. and DSc degrees in physics in 1989, 1997 and 2012, respectively. He has been working at the University of Szeged from 1994 to present, since 2013 as a professor. Since 2022 he is the principal investigator of the ELKH-SZTE Research Group for Photoacoustic Monitoring of Environmental Processes. He has been participated in the development and successful commercialization of photoacoustic instruments for various applications including oil and gas industry and environmental monitoring. For his innovations in the field of photoacoustics he has received various prizes including the Gábor Dénes Award in 2017.



Gábor Szabó is a full member of the Hungarian Academy of Sciences since 2010 and the Head of the Physics Doctoral School at University of Szeged since 2007. He has been working at the University of Szeged from 1978 to present, since 1994 as a professor. Since 2020 he is the Managing Director of ELI-ALPS. His research fields and interests include photoacoustic spectroscopy, ultrafast laser spectroscopy, generation of femtosecond pulses, nonlinear optics, control of quantum systems and applications of lasers in medicine.